Available online at www.sciencedirect.com
ScienceDirect
Journal of Solid State Chemistry 180 (2007) 799–803
JOURNAL OF SOLID STATE CHEMISTRY
www.elsevier.com/locate/jssc

Rapid communication

Ionic liquid of $[Bmim]^+Cl^-$ for the preparation of hierarchical nanostructured rutile titania

Ningya Yu[a,*], Liming Gong[a], Huijuan Song[a], Yong Liu[b], Donghong Yin[a,*]

[a]*Institute of Fine Catalysis & Synthesis, College of Chem. & Chem. Eng., Hunan Normal University, Changsha 410081, PR China*
[b]*Key Laboratory of Organosilicon Chemistry and Material Technology of Ministry of Education, Hangzhou Teachers College, Hangzhou 310012, PR China*

Received 11 August 2006; received in revised form 30 October 2006; accepted 6 November 2006
Available online 14 November 2006

Abstract

The rutile titania with hierarchical nanostructure was conveniently prepared in a room temperature ionic liquid (RTIL) of $[Bmim]^+Cl^-$ system. The obtained materials were characterized by powder X-ray diffraction (XRD), scanning electron microscopy (SEM), transmission electron microscopy (TEM), and N_2 adsorption–desorption analysis. XRD patterns revealed that only rutile phase was formed in the ionic liquid of $[Bmim]^+Cl^-$. The SEM and TEM micrographs as well as N_2 adsorption–desorption measurements showed that the nanorods of rutile titania were interaggregated to fabricate a large mesoporous structure and the voids packed in the nanorods formed a small mesostructure. It was proposed that the formation of rutile crystal phase was due to high acidity and high Cl^- content in the special reaction media, and also the combination of ionic liquid-templated effects with so-called reaction limited aggregation resulted in the hierarchical nanostructure.

Keywords: TiO_2; Ionic liquid; Rutile; Nanostructure

1. Introduction

Because of its excellent physical and chemical properties including photocatalysis, sensitivity to humidity and gas, dielectric character, photo-electrochemical conversion, etc., TiO_2 has received considerable attention in several scientific disciplines [1–3]. It is well-established that TiO_2 exists in three main crystalline forms (i.e., anatase, rutile, and brookite) and that each crystalline structure exhibits different physicochemical properties. In general, anatase TiO_2 possesses higher electrochemical performance than rutile phase, whereas rutile TiO_2 has higher chemical stability and refractive index. For some advanced applications of TiO_2, for example, the preparation of nanodevice and nanosensor, besides crystalline structure, morphology of TiO_2 plays a crucial role in properties of ultimate product. Thus, it is practically and scientifically significant to explore new synthetic methods to fabricate nanostructured TiO_2 with specific crystalline structure. Recently, there has been a great deal of research on the preparation of nanostructured TiO_2 [4–14]. In comparison with the synthesis of nanostructured anatase, however, the preparation of rutile with ultrafine nanostructure has scarcely been reported in spite of its important application in optical communication [9–14]. The fact is that the synthesis of monomineralic, well-shaped rutile nanostructure is much more difficult than the synthesis of anatase nanocrystals. Indeed, the much lower surface energy of anatase, relative to rutile, often results in a reversal in thermodynamic stabilities in the limit of very small nanostructures [15].

More recently, the advantages of room temperature ionic liquids (RTILs) for materials chemistry and especially for the synthesis of novel nanostructures have been realized [16–25]. There have reports on the formation of anatase TiO_2 nanocrystals [4], hollow TiO_2 microspheres [17], CuCl nanoplatelets [18], sulfide M_2S_3 (M = Bi, Sb) nanorods [20], CoPt nanorods [21], $PbCrO_4$ and Pb_2CrO_5 rods [25] in RTIL-containing media. Such synthetic systems showed unprecedented advantages [26]: (1) hydroxide and oxihydrate formation can be suppressed, which facilitates direct

*Corresponding authors. Fax: +86 731 8872531.
E-mail addresses: yuningya@yahoo.com.cn (N. Yu), yindh@hunnu.edu.cn (D. Yin).

0022-4596/$ - see front matter © 2006 Elsevier Inc. All rights reserved.
doi:10.1016/j.jssc.2006.11.008

synthesis of crystalline structures at low temperature; (2) low interface tensions of RTILs lead to high nucleation rates and, thus, products with nano-scale can be easily generated; (3) more importantly, the self-structuration of RTILs originated from the extended H-bond systems make RTILs suitable as template for the synthesis of inorganic materials with ultrafine nanostructure. Until now, unfortunately, the crystal type of nanostructured TiO_2 prepared in RTILs is not rutile but anatase [4,22–24], which may be due to the fact that the fast crystallization at room temperature encourages the formation of anatase [27]. Since the high acidity and concentration of Cl^- usually result in the formation of rutile phase [28,29], Cl^--containing RTILs should be a promising candidate to the preparation of nanostructured rutile TiO_2 under high acidity condition. In this work, a direct soft synthesis of clean rutile with a unique hierarchical nanostructure in a RTIL of $[Bmim]^+Cl^-$ medium was reported. The novel method avoided high temperature treatments that usually alter the nanostructure because of volume and shape changes.

2. Experimental

2.1. Materials

1-Methylimidazole, 1-Chlorobutane and $TiCl_4$ were purchased from ACROS. Other commercially available chemicals were laboratory grade reagents from local suppliers. All the chemicals were used as received.

2.2. Synthesis

Ionic liquid of $[Bmim]^+Cl^-$ was prepared as previously reported [30]. Prior to use, the RTIL was dried by heating under vacuum.

The hierarchical nanostructured rutile titania was synthesized as follows: 2 mL of $TiCl_4$, 4 mL of deionized H_2O and 5.5 g of $[Bmim]^+Cl^-$ were mixed at 0 °C under stirring, followed by stirring at 80 °C for 4 h, then the obtained dispersion was diluted with 20 mL of deionized H_2O. The resulting precipitate was gathered by centrifugation. In order to improve the crystallinity of product and to control the grain size, the obtained precipitate underwent hydrothermal treatment by being put into a Teflon-lined autoclave containing 30 mL of water and heated at 80, 120 or 160 °C for 12 h, respectively. The residual of RTIL in the product was removed by extracting the sample with acetonitrile in a Teflon-lined autoclave at 50 °C for 24 h. The extraction process was repeated until the C–H stretching region (around 2900 cm^{-1}) of $[Bmim]^+Cl^-$ disappeared completely [22]. The final product was dried in a rotational evaporator at 50 °C and then ground to fine powder. The sample without hydrothermal aging was denoted as S_R and the samples with hydrothermal aging at 80, 120, 160 °C were denoted as S_R-80, S_R-120, and S_R-160, respectively.

2.3. Characterization

Powder X-ray diffraction (XRD) patterns of the samples were measured on a Rigaku D/max 2500V/PC diffractometer using Cu$K\alpha$ radiation. N_2 adsorption–desorption analyses of the samples were measured at −196 °C on a Micromeritics Tristar 3000 sorptometer. Prior to the measurement, all samples were outgassed at 120 °C and 10^{-6} mmHg overnight. The surface areas were calculated by BET method, and the pore diameter distributions were determined from the adsorption branch of the isotherms using BJH method. Scanning electron microscopy (SEM) images were recorded on a JSM 6700F microscope. The samples were sputtered with gold prior to imaging. Transmission electron microscopy (TEM) images were observed on a JEOL 2010 microscope. The samples were

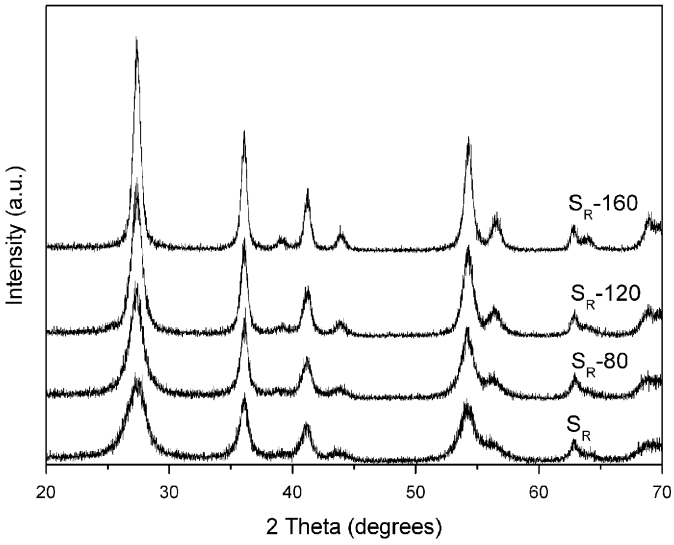

Fig. 1. XRD patterns of the S_R, S_R-80, S_R-120, and S_R-160.

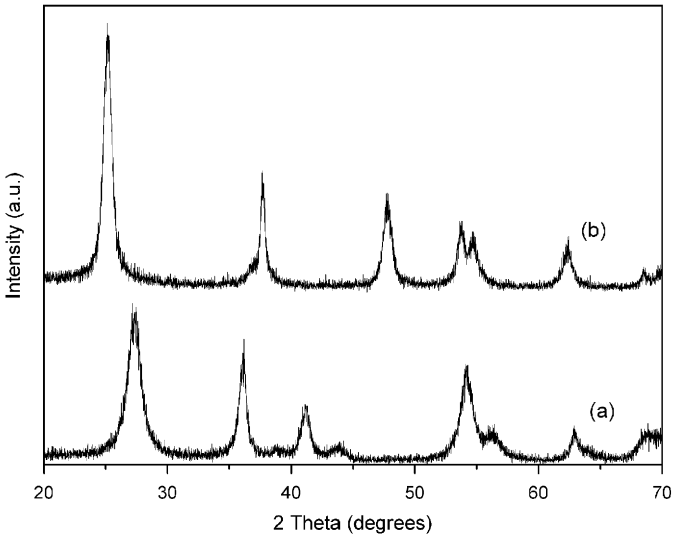

Fig. 2. XRD patterns of the S_R-80 (a) and S_A-80 (b).

scattered by ultrasonics for 15 min in ethanol, and two drops were taken onto carbon-coated copper grids.

3. Results and discussion

X-Ray diffraction patterns of the S_R, S_R-80, S_R-120, and S_R-160 are shown in Fig. 1. It was easily seen that the XRD data for the S_R was good match to the standard rutile pattern (JCPDS. No. 65-0191) and did not show any weak peaks at 25° or 31°, indicating that this sample is free of both anatase and brookite TiO_2 crystal phases. After the hydrothermal aging, the crystalline structure of the S_R was not changed and the crystallinity was improved with the increased aging temperature. These results are very interesting because RTILs facilitated direct synthesis of anatase phase at low temperature rather than rutile phase [4,22–24]. The formation of rutile phase should be attributed to the special reaction media presented here. It is

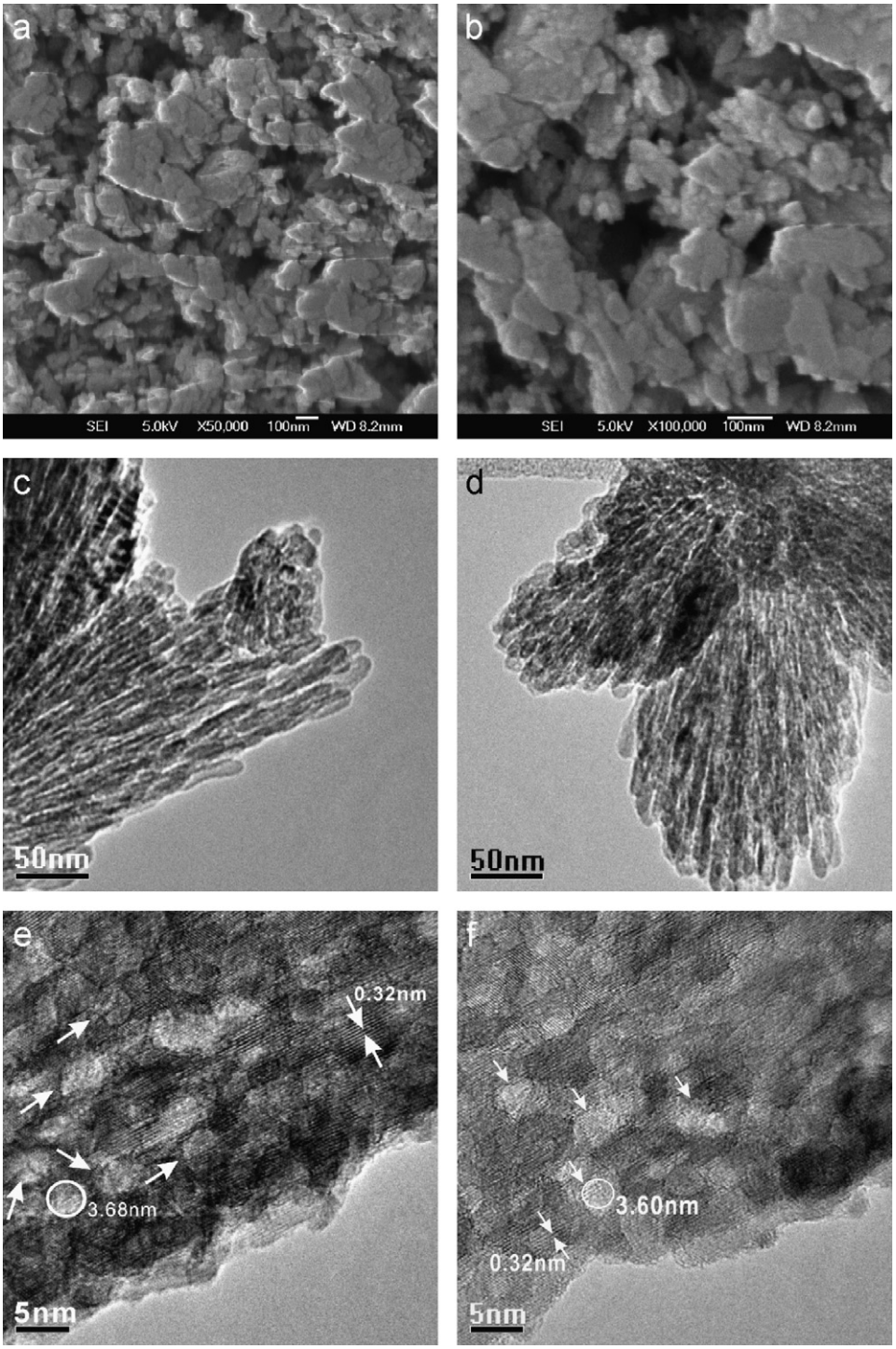

Fig. 3. SEM (a and b) and TEM (c–f) micrographs of the sample of S_R-120.

believed that Ti^{4+} ions are all octahedrally coordinated with the ligands of OH^- and Cl^- by forming chloride complexes of the type $[Ti(OH)_mCl_n]^{2-}$ under the conditions of high acidity and high Cl^- content [28], where $m+n=6$ and n is related with the concentration of Cl^- in synthetic system, i.e., the higher $[Cl^-]$, the bigger is n. During the condensation process via the dehydration reaction between OH ligands in $[Ti(OH)_mCl_n]^{2-}$, high value of n in $[Ti(OH)_mCl_n]^{2-}$ complexes will favor the formation of corner-sharing titanium-oxygen octahedrons by forming dimers and trimers, and, finally, the formation of rutile lattice [29]. It should be noted that, under otherwise the same conditions, the replacement of $[Bmim]^+Cl^-$ by $[Bmim]^+[BF_4]^-$ gave TiO_2 with anatase phase only (denoted as S_A-80, see Fig. 2), indicating that the Cl^- concentration in synthetic system plays a significant role in the crystalline structure of the final products. Therefore, the crystalline structure of TiO_2 prepared in RTIL-containing media can be controlled by the choice of various RTILs. By analyzing the diffraction line widths of the samples with pure rutile phase, it was found that the (110) peak was broader in width than the others, implying that epitaxial growth might have occurred. The average grain sizes of the S_R, S_R-80, S_R-120, and S_R-160 were 6.5, 8.1, 10.4, and 13.4 nm, respectively, determined from the broadening of (1 1 0) peak using the Scherrer formula.

Fig. 3 shows the SEM and TEM images of the S_R-120. The stacks of irregularly shaped particles with unsmooth surfaces were observed in the SEM observations (see Fig. 3(a)). A higher magnification image shown in Fig. 3(b) revealed that many elongated particles formed on the surface. This suggests that the particles grow anisotrophically, which is consistent with the results of XRD. The TEM micrographs shown in Fig. 3(c) and (d) gave a clear observation of the particles, in which the particles were comprised of interaggregated nanorods with a diameter of about 10 nm. The diameter of the nanorods observed in TEM images were the same as the average particle size (10.4 nm) calculated from the peak broadening by the Scherrer formula. Moreover, voids with the size of 3.7 nm packed in nanorods were observed in the high magnification image (Fig. 3(e) and (f)), which formed a mesostructure without discernible long-range order. Also, lattice images parallel to the nanorods could be seen in the high magnification image. The distance between the adjacent lattice fringes was estimated to be 0.32 nm, which is an indication that the crystal growth is preferential in the [110] direction [10].

In order to further describe the nanostructures of the aged rutile samples, the N_2 adsorption–desorption characterization was performed and the corresponding results are shown in Fig. 4 and Table 1. Clearly, the pore size distributions of all samples were bimodal (see Fig. 4), suggesting that these samples possess a bimodal hierarchical porosity. The small mesopores could correspond to the voids packed in the nanorods. Indeed, in the case of the sample of S_R-120, the small pore size observed in the TEM

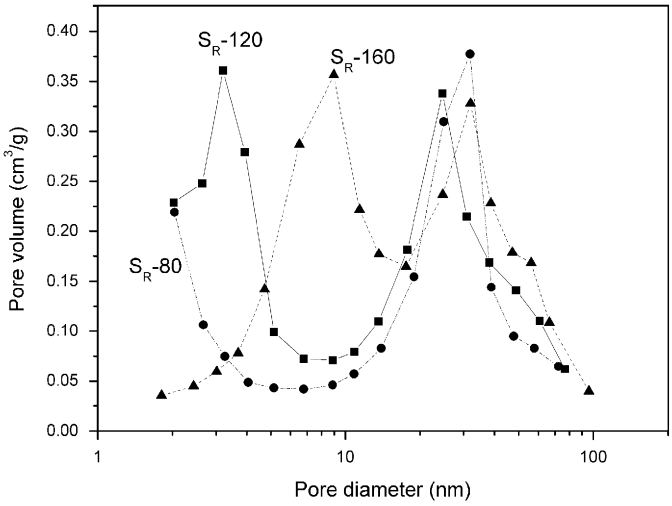

Fig. 4. Pore size distributions of the S_R-80, S_R-120, and S_R-160.

Table 1
Textural properties of the samples aged at different temperature

Aging temp. (°C)	S_{BET} ($m^2 g^{-1}$)	V_P ($cm^3 g^{-1}$)	D_{BJH} (nm)	
80	173	0.21	~2	32
120	169	0.25	3.2	25
160	96	0.27	9.0	32

image was consistent with the value measured by N_2 adsorption–desorption (3.7 nm vs. 3.2 nm). The large mesopores should correspond to the interaggregation of nanorods. Moreover, elevated aging temperature led to an increasing pore size of small mesopores and a decrease of the specific surface area, which is probably due to the growth of TiO_2 crystallites via ostwald ripening. However, the value of total pore volume did not decrease with the increase of aging temperature, indicating that the increased aging temperature does not result in the collapse of the pore system. It should be noted that the pore size of small mesopores could be easily adjusted by choosing hydrothermal treatment temperature.

Although a glimpse of the change in the crystal structures could be understood, the formation of the bimodal nanopores still remained elusive to us. Here, we attributed small mesopores to the aggregation of $[Bmim]^+Cl^-$ [31]. RTILs with sufficiently long alkyl chains (such as C_4) have been found to preferentially assemble in a so-called tail-to-tail fashion with the head representing the imidazole moiety and the tail representing the alkyl chain [32,33]. Recently, Wang et al. have used a multiscale coarse-graining (MS-CG) method to explore the effect of various cation side-chain lengths on the self-assembly of $[C_nmim]^+[NO_3]^-$. It was found that the charged anions and headgroups of the cations distribute homogeneously because of the strong electrostatic interactions and that the

neutral tail groups tend to aggregate due to the collective short-range interaction [34]. The formation of large mesopores should be due to so-called reaction limited aggregation (RLA), which has been proposed to lead to the formation of mesostructure [4]. Nevertheless, further investigations have to be carried out to get further understanding of the formation mechanism of the present TiO_2 hierarchical nanostrucutre.

4. Conclusion

In summary, the ionic liquid of $[Bmim]^+Cl^-$ was employed to prepare rutile titania with hierarchical nanostructure, in which the nanorods were interaggregated to fabricate a large mesoporous structure and the voids packed in the nanorods formed smaller mesostructure. The small mesopores were provisionally attributed to the aggregation of the RTIL, whereas the large elongated mesopores origined from the reaction limited aggregation. Furthermore, the pore size of small mesopores could be easily adjusted by changing the hydrothermal treatment temperature.

Acknowledgments

The project sponsored by the Scientific Research Foundation for the Returned Overseas Chinese Scholars, Ministry of Education [2003-406].

References

[1] M.R. Hoffmann, S.T. Martin, W. Choi, D.W. Bahnemann, Chem. Rev. 95 (1995) 69.
[2] D. Yin, M. Komiyama, Jpn. J. Appl. Phys. 40 (2001) 4281.
[3] U. Diebold, Surf. Sci. Rep. 48 (2003) 53.
[4] Y. Zhou, M. Antonietti, J. Am. Chem. Soc. 125 (2003) 14960.
[5] Y. Lan, X.P. Gao, H.Y. Zhu, Z.F. Zheng, T.Y. Yan, F. Wu, S.P. Ringer, D.Y. Song, Adv. Funct. Mater. 15 (2005) 1310.
[6] A. Chemseddine, T. Moritz, Eur. J. Inorg. Chem. (1999) 235.
[7] Z.Y. Yuan, T.Z. Ren, B.L. Su, Adv. Mater. 15 (2003) 1462.
[8] J.L. Blin, A. Leonard, Z.Y. Yuan, L. Gigot, A. Vantomme, A.K. Cheetham, B.L. Su, Angew. Chem. Int. Edit. 42 (2003) 2872.
[9] Y.Z. Li, N.H. Lee, E.G. Lee, J.S. Song, S.J. Kim, Chem. Phys. Lett. 389 (2004) 124.
[10] Q. Huang, L. Gao, Chem. Lett. 32 (2003) 638.
[11] D.B. Kuang, A.W. Xu, J.Y. Zhu, H.Q. Liu, B.S. Kang, New J. Chem. 26 (2002) 819.
[12] K. Yang, J.M. Zhu, J.J. Zhu, S.S. Huang, X.H. Zhu, G.B. Ma, Mater. Lett. 57 (2003) 4639.
[13] X. Li, Y. Xiong, Z. Li, Y. Xie, Inorg. Chem. 45 (2006) 3493.
[14] Q.H. Zhang, L. Gao, Langmuir 19 (2003) 967.
[15] H. Zhang, J.F. Banfield, J. Mater. Chem. 8 (1998) 2073.
[16] M. Antonietti, D. Kuang, B. Smarsly, Y. Zhou, Angew. Chem. Int. Ed. 43 (2004) 4988.
[17] T. Nakashima, N. Kimizuka, J. Am. Chem. Soc. 125 (2003) 6386.
[18] A. Taubert, Angew. Chem. Int. Ed. 43 (2004) 5380.
[19] Y. Zhou, J.H. Schattka, M. Antonietti, Nano Lett. 4 (2004) 477.
[20] Y. Jiang, Y.J. Zhu, J. Phys. Chem. B 109 (2005) 4361.
[21] Y. Wang, H. Yang, J. Am. Chem. Soc. 127 (2005) 5316.
[22] K. Yoo, H. Choi, D.D. Dionysiou, Chem. Commun. (2004) 2000.
[23] K. Yoo, T.G. Lee, J. Kim, Micropor. Mesopor. Mater. 84 (2005) 211.
[24] Y. Liu, J. Li, M.J. Wang, Z.Y. Li, H.T. Liu, P. He, X.R. Yang, J.H. Li, Cryst. Growth Des. 5 (2005) 1643.
[25] W.W. Wang, Y.J. Zhu, Cryst. Growth Des. 5 (2005) 505.
[26] M. Antonietti, D. Kuang, B. Smarsly, Y. Zhou, Angew. Chem. Int. Ed. 43 (2004) 4988.
[27] F. Bosc, A. Ayral, P.A. Albouy, C. Guizard, Chem. Mater. 15 (2003) 2463.
[28] H. Cheng, J. Ma, Z. Zhao, L. Qi, Chem. Mater. 7 (1995) 663.
[29] G.S. Li, L.P. Li, J.B. Goates, B.F. Woodfield, J. Mater. Res. 18 (2003) 2664.
[30] J.G. Huddleston, H.D. Willauer, R.P. Swatloski, A.E. Visser, R.D. Rogers, Chem. Commun. (1998) 1765.
[31] Y. Zhou, M. Antonietti, Chem. Mater. 16 (2004) 544.
[32] T.L. Merrigan, E.D. Bates, S.C. Dorman, J.H. Davis, Chem. Commun. (2000) 2051.
[33] S. Dorbritz, W. Ruth, U. Kragl, Adv. Synth. Catal. 347 (2005) 1273.
[34] Y.T. Wang, G.A. Voth, J. Am. Chem. Soc. 127 (2005) 12192.